Eur. Phys. J. Plus (2022) 137:610
https://doi.org/10.1140/epjp/s13360-022-02735-2

THE EUROPEAN PHYSICAL JOURNAL PLUS

Regular Article

Rashba effect in a quantum dot subject to a parabolic confining potential and external fields

I. F. I. Mikhail[a], **I. M. M. Ismail, M. M. El Shafee**

Department of Mathematics, Faculty of Science, Ain Shams University, Cairo, Egypt

Received: 29 December 2021 / Accepted: 18 April 2022

Abstract The Rashba effect has been investigated in a spherical quantum dot confined by a radial parabolic potential. Also, external parallel magnetic and electric fields have been applied. The solution of the Schrödinger equation in the presence of the Rashba interactions has been derived by applying an approach that differs from the one used in an earlier treatment. The wave function in the presence of these interactions has been expanded in terms of the eigenfunctions of the Hamiltonian in their absence. In our opinion, the form introduced for the wave function presents the exact solution in a more accurate manner. The coefficients of expansion have been chosen either to depend on the three quantum numbers involved or on the principal quantum number only. The results have shown that the Rashba interactions have a considerable effect on the electron energy levels and on their splitting. The variation of this effect with the applied fields and the Rashba coupling strength has been investigated.

1 Introduction

Nowadays, the spin orbit interactions have gained a great attention in low-dimensional structures from both the theoretical and experimental points of view. The three main types of spin orbit interactions are conventional, Dresselhaus and Rashba interactions.

The conventional interactions result naturally due to the motion of the electron in its orbit. This motion, in turn, causes a coupling between the electron spin and its angular momentum (Griffiths [1] and Shankar [2]). Very few studies have been considered to explore such interactions in low-dimensional structures. Mikhail et al. [3, 4] have recently investigated this type of interactions in single and multilayered quantum dots in the presence of central and off-central impurities.

The Dresselhaus interactions (Dresselhaus [5]) result in crystals which possess a lack of symmetry under reflection about a plane that involves at least one lattice point. They have been studied by Lu and Li [6] in the presence of a magnetic field and by Vaseghi et al. [7] in the presence of a spatial electric field.

The Rashba interactions (Rashba [8, 9]) are the most important type of spin orbit interactions that occur in low-dimensional structures. They occur in two-dimensional geometries. Their coupling coefficient is much higher than that of Dresselhaus interactions. They mainly depend on the inversion symmetry breaking in the direction perpendicular to the two-dimensional structure. They have been investigated in two-dimensional electron systems such as quantum discs [10–13]. They have further been investigated in a two-dimensional electron gas in the presence of an external magnetic field. The study has been extended to explore the magneto-quantum transport and magneto-thermodynamics properties of the system [14–19]. The Rashba interactions have also been investigated under the effect of electric and magnetic fields in a one-dimensional parabolic confinement quantum well wire [20–22] and in a two-dimensional electron system (Papp and Micu [23]). The same problem was also studied on a circular cylinder of constant radius (Mehdiyev et al. [24]) and in a spherical quantum dot by Vaseghi et al. [25, 26].

Moreover, the linear and third-order nonlinear optical properties in the presence of Rashba interactions have been investigated in low-dimensional structures by many authors [20, 26–33]. Also, the effect of the Rashba interactions on the binding energy of a hydrogenic impurity has been considered by Vanitha et al. [34] in a quantum well and by Safaei et al. [35] in quantum nanowires. Furthermore, the Rashba effect has been studied by Sainy et al. [36] in a two-dimensional Gaussian GaAs quantum dot in the presence of a central impurity and an external magnetic field.

The present work is concerned with studying the effect of the Rashba spin orbit interactions in the presence of external magnetic and electric fields in a radial parabolic confinement spherical quantum dot. The same problem was previously considered by Vaseghi et al. [25, 26]. In Refs. [25, 26], the eigenfunction in the presence of Rashba interactions was taken in the same form as Mehdiyev et al. [24]. This form depends on one eigenfunction of the Hamiltonian operator in the absence of the Rashba interaction. It was valid in Mehdiyev et al. [24] since they have considered a circular cylinder of constant radius ρ. Accordingly, it is also an eigenfunction of the spin orbit operator and of the total Hamiltonian. However, in the case of a spherical quantum dot the polar coordinate ρ varies and

[a] e-mail: ifi_mikhail@hotmail.com (corresponding author)

Published online: 20 May 2022

accordingly the suggested form is not a suitable choice for the eigenfunction after taking the Rashba effect into consideration. In the present work, an alternative approach has been applied. We have expanded the wave function of the total Hamiltonian after including the Rashba effect as a linear combination of the eigenfunctions of the Hamiltonian in the absence of the Rashba interactions. Similar approaches have been applied hitherto in other problems, for example by Akbari et al. [37] to study the spin orbit interactions in a two-dimensional quantum pseudo-dot system and by Shakouri et al. [38] to investigate these interactions in a quasi-one-dimensional quantum rings.In the present work, the coefficients of the expansion have been taken either to depend on the three quantum numbers involved or to depend only on the principal quantum number. In the latter case, one-band and two-band models have been considered. The results have been applied to the case of GaAs spherical quantum dot. The change of the lower energy eigenvalues due to the Rashba interactions has been investigated. The variation of the Rashba effect has been studied with the applied magnetic field, the electric field, and with the strength of the Rashba coupling.

The paper is organized as follows: The basic equations are considered in Sect. 2, where the forms of the Hamiltonian and the Rashba spin orbit operators have been given as well as the forms of the eigenfunctions and eigenvalues in the absence of the Rashba interactions. The general expansion solution in the presence of the Rashba interactions is presented in Sect. 3. Regarding, the coefficients of the expansion two alternative assumptions have been utilized. In Sect. 4, they have been taken to depend on the three quantum numbers involved while in Sect. 5, they have been taken to depend only on the principal quantum number. In the latter case, two models have been explored, namely the one-band and the two-band models. Finally the numerical results obtained for a GaAs quantum dot are discussed in Sect. 6.

2 Basic equations

The Hamiltonian operator of an electron in a spherical quantum dot confined by a radial parabolic potential in the form $\frac{1}{2}m^*\omega_o^2 r^2$ under the influence of external electric and magnetic fields with Rashba spin orbit interaction (SOI) can be represented by

$$\hat{H} = \hat{H}_o + \hat{H}_{SO}, \tag{1}$$

where in cylindrical coordinates

$$\hat{H}_o = -\frac{\hbar^2}{2m^*}\left(\frac{1}{\rho}\frac{\partial}{\partial\rho}\left(\rho\frac{\partial}{\partial\rho}\right) + \frac{\partial^2}{\partial z^2} + \frac{1}{\rho^2}\frac{\partial^2}{\partial\phi^2}\right) + \frac{1}{2}\omega_c\hat{L}_z + \frac{m^*\Omega^2\rho^2}{8} - eFz + \frac{m^*\omega_o^2 z^2}{2}. \tag{2}$$

In the above equation ω_o is the angular frequency that determines the confined potential, $\widehat{L}_z$ is the component of the angular momentum along the direction of the magnetic field $\boldsymbol{B}$, m^* is the electron effective mass, $\boldsymbol{F}$ is the electric field, ω_c is the cyclotron frequency defined by

$$\omega_c = \frac{eB}{m^*}, \tag{3}$$

and

$$\Omega = \sqrt{\omega_c^2 + 4\omega_o^2}. \tag{4}$$

It is worthwhile pointing out that the use of cylindrical coordinates in Eq. (2) is valid since the parabolic potential is extended to infinity and accordingly no boundary conditions have to be applied at the surface of the sphere.

The Rashba SOI Hamiltonian in an external magnetic field $\boldsymbol{B}$ applied along the$z$-axis is given by

$$\hat{H}_{\mathrm{SO}} = \frac{\alpha}{\hbar}\Big(\boldsymbol{\sigma} \times \Big(\hat{\boldsymbol{P}} + \mathrm{e}\boldsymbol{A}\Big)\Big).\boldsymbol{n}, \tag{5}$$

where $\widehat{\boldsymbol{P}}$ is the momentum operator, α is the strength of the Rashba interaction, $\boldsymbol{\sigma} = (\sigma_x, \sigma_y, \sigma_z)$ denotes the Pauli spin matrices, $\boldsymbol{n}$ is normal to the surface and $\boldsymbol{A}$ is the vector potential. The normal to the surface is taken to be

$$\boldsymbol{n} = -\boldsymbol{e}_\rho = -\cos(\phi)\boldsymbol{i} - \sin(\phi)\boldsymbol{j}, \tag{6}$$

in Cartesian coordinates. Also, using the symmetric Landau gauge, $\boldsymbol{A}$ takes the form

$$\boldsymbol{A} = \frac{B}{2}(-y, x, 0), \tag{7}$$

$$\boldsymbol{A} = \left(A_\rho = 0, A_\phi = \frac{B\rho}{2}, A_z = 0\right). \tag{8}$$

Equations (7), and (8) give the components of $\boldsymbol{A}$ in Cartesian and cylindrical polar coordinates, respectively. It, then, follows from Eq. (5) that $\widehat{H}_{so}$ can be expressed in cylindrical polar coordinates

$$\hat{H}_{\mathrm{SO}} = -\frac{i\alpha}{\rho}\frac{\partial}{\partial\phi}\sigma_z + i\alpha\cos(\phi)\frac{\partial}{\partial z}\sigma_y - i\alpha\sin(\phi)\frac{\partial}{\partial z}\sigma_x + \frac{\alpha eB\rho}{2\hbar}\sigma_z. \tag{9}$$

Now, the Schrödinger equation corresponding to the Hamiltonian operator $\widehat{H}_o$ is given by

$$\hat{H}_o\Psi = E_o\Psi. \tag{10}$$

The separation of variables technique implies consequently

$$\psi_{nmn_z}(\rho,\phi,z) = \frac{1}{\sqrt{2\pi}}e^{im\phi}f_{nm}(\rho)G_{n_z}(z), \tag{11}$$

where n, m, n_z are the radial, magnetic and azimuthal quantum numbers which result due to the solution of the Schrödinger Eq. (10). It can be shown by substituting from Eq. (11) in Eq. (10) that $f_{nm}(\rho)$ can be expressed as

$$f_{nm}(\rho) \equiv f_{nm}(\zeta) = \frac{1}{a}\sqrt{\frac{n!}{(n+|m|)!}}e^{\frac{-\zeta}{2}}\zeta^{\frac{|m|}{2}}L_n^{|m|}(\zeta), \tag{12}$$

where $L_n^{|m|}(\zeta)$ is the associated Laguerre polynomial and

$$a = \sqrt{\frac{\hbar}{m^*\Omega}}, \quad \zeta = \frac{\rho^2}{2a^2}. \tag{13}$$

Also, $G_{n_z}(z)$ takes the form

$$G_{n_z}(z) = \sqrt{\frac{W}{\pi^{1/2}2^{n_z}n_z!}}e^{-\frac{1}{2}X^2}H_{n_z}(X), \tag{14}$$

where $H_{n_z}(X)$ is the Hermite polynomial and

$$W = \sqrt{\frac{m^*\omega_o}{\hbar}}, X = W(z-z_o), z_o = \frac{eF}{m^*\omega_o^2}. \tag{15}$$

The corresponding energy eigenvalues of $\widehat{H}_o$ are accordingly given by

$$E_{o(n,m,n_z)} = \hbar\Omega\left(n+\frac{1+|m|}{2}\right)+\frac{m\hbar\omega_c}{2}+\hbar\omega_o\left(n_z+\frac{1}{2}\right)-\frac{e^2F^2}{2m^*\omega_o^2}. \tag{16}$$

3 The general expansion solution

The Schrödinger equation corresponding to the total Hamiltonian $\widehat{H}$ (Eq. 1) takes the form

$$\hat{H}\Psi = E\Psi. \tag{17}$$

In Vaseghi et al. [25, 26], Ψ has been taken in the form $e^{\pm\frac{1}{2}i\phi}\psi$, where ψ is one of the eigenfunctions of H_o while the term $e^{\pm\frac{1}{2}i\phi}$ represents the spinor S_z. It is readily shown that the resulting form of Ψ is not an eigenfunction of $\widehat{H}_{SO}$ and of $\widehat{H}$. It seems that this procedure is invalid for the present calculations. In fact, Vaseghi et al. [25, 26] have resembled the calculations of Mehdiyev et al. [24]. However, in Ref. [24], the situation was entirely different as the study was performed for a circular cylinder of constant radius ρ.

Here, we apply an alternative approach in which the eigenfunctions $\psi_{nmn_z}(\rho,\phi,z)$ of $\widehat{H}_o$ will be taken as an orthonormal basis. Accordingly, the general solution $\Psi(\rho,\phi,z)$ of Eq. (17) can be expanded as

$$\Psi = \sum_{nmn_z}\psi_{nmn_z}(\rho,\phi,z)\left(C^+_{nmn_z}\Big|+>+C^-_{nmn_z}\Big|->\right). \tag{18}$$

The substitution of Eq. (18) in (17) and the comparison of the coefficients of $e^{im\phi}$ and $|+>, |->$ on both sides lead to the following two basic equations:

$$\sum_{nn_z}C^+_{nmn_z}\left(E_{onmn_z}-E+\frac{\alpha m}{a\sqrt{2\zeta}}+\frac{eB\alpha a\sqrt{\zeta}}{\sqrt{2}\hbar}\right)f_{nm}(\zeta)G_{n_z}(z)+\alpha\sum_{nn_z}C^-_{n(m+1)n_z}f_{n,m+1}(\zeta)\frac{d}{dz}\big(G_{n_z}(z)\big)=0. \tag{19}$$

and

$$-\alpha\sum_{nn_z}C^+_{n(m-1)n_z}f_{n,m-1}(\zeta)\frac{d}{dz}\big(G_{n_z}(z)\big)+\sum_{nn_z}C^-_{nmn_z}\left(E_{onmn_z}-E-\frac{\alpha m}{a\sqrt{2\zeta}}-\frac{eB\alpha a\sqrt{\zeta}}{\sqrt{2}\hbar}\right)f_{nm}(\zeta)G_{n_z}(z)=0. \tag{20}$$

It is readily shown that

$$\frac{d}{dz}\left(G_{n_z}(z)\right)=\sqrt{\frac{W}{\pi^{\frac{1}{2}}2^{n_z}n_z!}}W\left[n_zH_{n_z-1}(X)-\frac{1}{2}H_{n_z+1}(X)\right]e^{-\frac{1}{2}X^2}. \tag{21}$$

In deriving the above result, we have utilized the properties of the Hermite polynomial given in (Lebedev [39]). On substituting from Eq. (21) in Eqs. (19), (20), multiplying by $G_{n_z'}(z)$ and using the normalization conditions

$$\int_{-\infty}^{\infty}H_{n_z}(x)H_{n_z'}(x)e^{-x^2}dx=\delta_{n_zn_z'}\left(\pi^{\frac{1}{2}}2^{n_z}n_z!\right) \tag{22a}$$

and

$$\int_{-\infty}^{\infty}G_{n_z}(z)G_{n_z'}(z)dz=\delta_{n_zn_z'}, \tag{22b}$$

it can be shown after some algebra that

$$\begin{aligned}&\sum_n C^{+}_{nmn_z'}\left(E_{onmn_z'}-E+\frac{\alpha m}{a\sqrt{2\zeta}}+\frac{\alpha eBa}{\sqrt{2}\hbar}\sqrt{\zeta}\right)f_{nm}(\zeta)\\&+\frac{\alpha W}{\sqrt{2}}\sum_n\left[C^{-}_{n(m+1)\left(n_z'+1\right)}\sqrt{n_z'+1}-C^{-}_{n(m+1)\left(n_z'-1\right)}\sqrt{n_z'}\right]f_{n,m+1}(\zeta)=0\end{aligned} \tag{23}$$

and

$$\begin{aligned}&-\frac{\alpha W}{\sqrt{2}}\sum_n\left[C^{+}_{n(m-1)\left(n_z'+1\right)}\sqrt{n_z'+1}-C^{+}_{n(m-1)\left(n_z'-1\right)}\sqrt{n_z'}\right]f_{n,m-1}(\zeta)\\&+\sum_n C^{-}_{nmn_z'}\left(E_{onmn_z'}-E-\frac{\alpha m}{a\sqrt{2\zeta}}+\frac{\alpha eBa}{\sqrt{2}\hbar}\sqrt{\zeta}\right)f_{nm}(\zeta)=0.\end{aligned} \tag{24}$$

Equations (23), (24) are the most general two equations which relate the coefficients $C^{\pm}_{nmn_z}$ together. In the following two sections, we discuss two different approaches to deal with these coefficients.

4 The coefficients $C^{\pm}_{nmn_z}$ depend on all quantum numbers

Here we treat the problem with the coefficients of expansion depending on the three quantum numbers (n, m, n_z). We first replace m by $m+1$ in Eq. (24) to find

$$\begin{aligned}&-\frac{\alpha W}{\sqrt{2}}\sum_n\left[C^{+}_{nm\left(n_z'+1\right)}\sqrt{n_z'+1}-C^{+}_{nm\left(n_z'-1\right)}\sqrt{n_z'}\right]f_{nm}(\zeta)\\&+\sum_n C^{-}_{n(m+1)n_z'}\left(E_{on(m+1)n_z'}-E-\frac{\alpha(m+1)}{a\sqrt{2\zeta}}-\frac{\alpha eBa}{\sqrt{2}\hbar}\sqrt{\zeta}\right)f_{n(m+1)}(\zeta)=0.\end{aligned} \tag{25}$$

The second and third steps are to replace n_z' in Eq. (25) by $n_z'-1$ and $n_z'+1$. The resulting two equations are

$$\begin{aligned}&-\frac{\alpha W}{\sqrt{2}}\sum_n\left[C^{+}_{nmn_z'}\sqrt{n_z'}-C^{+}_{nm\left(n_z'-2\right)}\sqrt{n_z'-1}\right]f_{nm}(\zeta)\\&+\sum_n C^{-}_{n(m+1)\left(n_z'-1\right)}\left(E_{on(m+1)\left(n_z'-1\right)}-E-\frac{\alpha(m+1)}{a\sqrt{2\zeta}}-\frac{\alpha eBa}{\sqrt{2}\hbar}\sqrt{\zeta}\right)f_{n(m+1)}(\zeta)=0.\end{aligned} \tag{26}$$

and

$$\begin{aligned}&-\frac{\alpha W}{\sqrt{2}}\sum_n\left[C^{+}_{nm\left(n_z'+2\right)}\sqrt{n_z'+2}-C^{+}_{nmn_z'}\sqrt{n_z'+1}\right]f_{nm}(\zeta)\\&+\sum_n C^{-}_{n(m+1)\left(n_z'+1\right)}\left(E_{on(m+1)\left(n_z'+1\right)}-E-\frac{\alpha(m+1)}{a\sqrt{2\zeta}}-\frac{\alpha eBa}{\sqrt{2}\hbar}\sqrt{\zeta}\right)f_{n(m+1)}(\zeta)=0.\end{aligned} \tag{27}$$

For the lower energy levels, we take $m = 0, n_z^{'} = 0$. Also, for a certain energy band (certain value of n), we find from Eqs. (23), (26), (27) that

$$C_{n00}^{+}\left(E_{on00} - E + \frac{\alpha eBa}{\sqrt{2}\hbar}\sqrt{\zeta}\right) f_{n0}(\zeta) + \frac{\alpha W}{\sqrt{2}} C_{n11}^{-} f_{n1}(\zeta) = 0, \tag{28}$$

$$-\frac{\alpha W}{\sqrt{2}}\left(-C_{n0,-2}^{+}\right)\sqrt{-1} f_{n0}(\zeta) + C_{n1,-1}^{-}\left(E_{on1,-1} - E - \frac{\alpha}{a\sqrt{2\zeta}} - \frac{\alpha eBa}{\sqrt{2}\hbar}\sqrt{\zeta}\right) f_{n1} = 0 \tag{29}$$

and

$$-\frac{\alpha W}{\sqrt{2}}\left(C_{n02}^{+}\sqrt{2} - C_{noo}^{+}\right) f_{n0}(\zeta) + C_{n11}^{-}\left(E_{on11} - E - \frac{\alpha}{a\sqrt{2\zeta}} - \frac{\alpha eBa}{\sqrt{2}\hbar}\sqrt{\zeta}\right) f_{n1}(\zeta) = 0. \tag{30}$$

We only consider the successive coefficients. Thus, the coefficients $C_{n0,-2}^{+}$ in Eq. (29) and C_{n02}^{+} in Eq. (30) can be neglected. Accordingly, Eq. (29) implies that $C_{n1,-1}^{-} = 0$ in this type of calculations. Consequently, Eqs. (28), (30) imply that

$$C_{n00}^{+}\left(E_{on00} - E + \frac{\alpha eBa}{\sqrt{2}\hbar}\sqrt{\zeta}\right) f_{n0}(\zeta) + \frac{\alpha W}{\sqrt{2}} C_{n11}^{-} f_{n1}(\zeta) = 0 \tag{31}$$

and

$$\frac{\alpha W}{\sqrt{2}} C_{n00}^{+} f_{n0}(\zeta) + C_{n11}^{-}\left(E_{on11} - E - \frac{\alpha}{a\sqrt{2\zeta}} - \frac{\alpha eBa}{\sqrt{2}\hbar}\sqrt{\zeta}\right) f_{n1}(\zeta) = 0. \tag{32}$$

The functions $f_{nm}(\zeta)$ involved in Eqs. (31), (32) can be determined from Eq. (12). We further restrict ourselves to the case $n = 1$ which represents the possible lower energy levels related by Eqs. (31), (32). It can thus be shown from Eqs. (31), (32) that

$$C_{100}^{+}\left(E_{o100} - E + \frac{\alpha eBa}{\sqrt{2}\hbar}\sqrt{\zeta}\right) f_{10}(\zeta) + \frac{\alpha W}{\sqrt{2}} C_{111}^{-} f_{11}(\zeta) = 0 \tag{33}$$

and

$$\frac{\alpha W}{\sqrt{2}} C_{100}^{+} f_{10}(\zeta) + C_{111}^{-}\left(E_{o111} - E - \frac{\alpha}{a\sqrt{2\zeta}} - \frac{\alpha eBa}{\sqrt{2}\hbar}\sqrt{\zeta}\right) f_{11}(\zeta) = 0, \tag{34}$$

where

$$f_{10}(\zeta) = \frac{1}{a} e^{-\frac{\zeta}{2}} L_1(\zeta) \tag{35a}$$

and

$$f_{11}(\zeta) = \frac{1}{a\sqrt{2}} e^{-\frac{\zeta}{2}} \zeta^{\frac{1}{2}} L_1^1(\zeta). \tag{35b}$$

We, now, multiply Eq. (33) by $f_{10}(\zeta)$ and Eq. (34) by $f_{11}(\zeta)$ and integrate over $\rho d\rho = a^2 d\zeta$ from 0 to ∞. The resulting two equations are given by

$$C_{100}^{+}\left[E_{o100} - E + \frac{\alpha eBa}{\sqrt{2}\hbar} J_1\right] + \frac{\alpha W}{2} C_{111}^{-} J_2 = 0 \tag{36}$$

and

$$\frac{\alpha W}{2} C_{100}^{+} J_2 + C_{111}^{-}\left[E_{o111} - E - \frac{\alpha}{2a\sqrt{2}} J_3 - \frac{\alpha eBa}{2\sqrt{2}\hbar} J_4\right] = 0 \tag{37}$$

where

$$J_1 = \int_0^\infty e^{-\zeta}\sqrt{\zeta}(L_1(\zeta))^2 d\zeta,$$

$$J_2 = \int_0^\infty e^{-\zeta}\sqrt{\zeta} L_1(\zeta) L_1^1(\zeta) d\zeta,$$

$$J_3 = \int_0^\infty e^{-\zeta}\sqrt{\zeta}\left(L_1^1(\zeta)\right)^2 d\zeta$$

and

$$J_4 = \int_0^\infty e^{-\zeta}\zeta^{3/2}\left(L_1^1(\zeta)\right)^2 d\zeta. \tag{38}$$

The integrals given in Eq. (38) are obtained by substituting for $f_{10}(\zeta)$, $f_{11}(\zeta)$ from Eqs. (35a, b). Also, in deriving Eqs. (36), (37) we have used the orthonormality condition

$$a^2 \int_0^\infty f_{nm}(\zeta) f_{n'm}(\zeta) d\zeta = \delta_{nn'}. \tag{39}$$

Now, for a nontrivial solution of Eqs. (36), (37) the determinant of the coefficients C^+_{100}, C^-_{111} must vanish. Accordingly,

$$\left[E_{\text{o}100} - E + \frac{\alpha eBa}{\sqrt{2}\hbar} J_1\right]\left[E_{\text{o}111} - E - \frac{\alpha}{2a\sqrt{2}} J_3 - \frac{\alpha eBa}{2\sqrt{2}\hbar} J_4\right] - \left(\frac{\alpha W}{2} J_2\right)^2 = 0. \tag{40}$$

The roots of Eq. (40) determine the new energy levels which replace $E_{\text{o}100}$, $E_{\text{o}111}$ after taking the Rashba effect into consideration. The results are given and discussed in Sect. 6.

5 The coefficients $C^{\pm}_{nmn_z}$ depend only on the principal quantum number (n)

In this section, we proceed to investigate the possibility of choosing the coefficients of expansion in Eq. (18) to depend only on the principal (radial) quantum number n. We thus drop the dependence of the coefficients $C^{\pm}_{nmn'_z}$ on m, n'_z in Eqs. (23), (24). Also, for the lower involved energy levels we take $m = 0, n'_z = 0$ in these equations to find

$$\sum_n C_n^+\left(E_{\text{o}n00} - E + \frac{\alpha eBa}{\sqrt{2}\hbar}\sqrt{\zeta}\right) f_{n0}(\zeta) + \frac{\alpha W}{\sqrt{2}} \sum_n C_n^- f_{n1}(\zeta) = 0 \tag{41}$$

and

$$-\frac{\alpha W}{\sqrt{2}} \sum_n C_n^+ f_{n,-1}(\zeta) + \sum_n C_n^-\left(E_{\text{o}n00} - E - \frac{\alpha eBa}{\sqrt{2}\hbar}\sqrt{\zeta}\right) f_{n0}(\zeta) = 0. \tag{42}$$

The functions $f_{n0}(\zeta)$, $f_{n1}(\zeta)$ can be determined from Eq. (12). Also, it is readily shown from Eq. (12) that $f_{n,-1}(\zeta) = f_{n1}(\zeta)$. Consequently, we multiply both Eqs. (41), (42) by $f_{n'0}(\zeta)$ and integrate over $\rho d\rho = a^2 d\zeta$ from 0 to ∞. Hence,

$$C_{n'}^+(E_{\text{o}n'00} - E) + \sum_n C_n^+ \frac{\alpha eBa}{\sqrt{2}\hbar} I_{n'n} + \frac{\alpha W}{\sqrt{2}} \sum_n \frac{C_n^-}{\sqrt{n+1}} \text{K}_{n'n} = 0 \tag{43}$$

and

$$-\frac{\alpha W}{\sqrt{2}} \sum_n \frac{C_n^+}{\sqrt{n+1}} \text{K}_{n'n} + C_{n'}^-(E_{\text{o}n'00} - E) - \frac{\alpha eBa}{\sqrt{2}\hbar} \sum_n C_n^- I_{n'n} = 0, \tag{44}$$

where

$$I_{n'n} = \int_0^\infty e^{-\zeta}\sqrt{\zeta} L_{n'}(\zeta) L_n(\zeta) d\zeta = I_{nn'}$$

and

$$\text{K}_{n'n} = \int_0^\infty e^{-\zeta}\sqrt{\zeta} L_{n'}(\zeta) L_n^1(\zeta) d\zeta. \tag{45}$$

It is of importance to point out that the integrals J_1, J_2 used in the previous section are equivalent to the integrals I_{11}, K_{11}, respectively.

5.1 One-band model

In this model, we consider only the terms due to certain $n, n^{'}$ in Eqs. (43), (44). Thus, for $n = n^{'} = 1$ we take into account the first term that results from the summations in these equations to find

$$C_1^+\left(E_{o100} - E + \frac{\alpha eBa}{\sqrt{2}\hbar} I_{11}\right) + \frac{\alpha W}{2} C_1^- \mathrm{K}_{11} = 0 \tag{46}$$

and

$$-\frac{\alpha W}{2} C_1^+ \mathrm{K}_{11} + C_1^-\left(E_{o100} - E - \frac{\alpha eBa}{\sqrt{2}\hbar} I_{11}\right) = 0 \tag{47}$$

For a nontrivial solution, it can be shown that

$$E_{o100} - E = \pm\sqrt{\left(\frac{\alpha eBa}{\sqrt{2}\hbar} I_{11}\right)^2 - \left(\frac{\alpha W}{2}\mathrm{K}_{11}\right)^2}. \tag{48}$$

The integrals I_{11}, K_{11} can be replaced by J_1, J_2 as was pointed out above. Moreover, Eq. (48) restricts the value of the magnetic field (B) to be higher than a certain lower limit for the quantity under the square root in Eq. (48) to be positive.

5.2 Two-band model

In the two-band model, we extend the results of the one band model and first take $n^{'} = 1$ in Eqs. (43), (44), and consider the terms $n = 1, 2$ from the summations in these equations. Also, the energy E_{o100} will be denoted by E_{o1} for simplicity. The resulting two equations are accordingly given by

$$\left[E_{o1} - E + \frac{\alpha eBa}{\sqrt{2}\hbar} I_{11}\right] C_1^+ + \left[\frac{\alpha W}{2}\mathrm{K}_{11}\right] C_1^- + \left[\frac{\alpha eBa}{\sqrt{2}\hbar} I_{12}\right] C_2^+ + \left[\frac{\alpha W}{\sqrt{6}}\mathrm{K}_{12}\right] C_2^- = 0 \tag{49}$$

and

$$\left[-\frac{\alpha W}{2}\mathrm{K}_{11}\right] C_1^+ + \left[E_{o1} - E - \frac{\alpha eBa}{\sqrt{2}\hbar} I_{11}\right] C_1^- - \left[\frac{\alpha W}{\sqrt{6}}\mathrm{K}_{12}\right] C_2^+ - \left[\frac{\alpha eBa}{\sqrt{2}\hbar} I_{12}\right] C_2^- = 0. \tag{50}$$

We then take $n^{'} = 2$ in Eqs. (43), (44), consider the terms for $n = 1, 2$ and denote E_{o200} by E_{o2} to find

$$\left[\frac{\alpha eBa}{\sqrt{2}\hbar} I_{21}\right] C_1^+ + \left[\frac{\alpha W}{2}\mathrm{K}_{21}\right] C_1^- + \left[E_{o2} - E + \frac{\alpha eBa}{\sqrt{2}\hbar} I_{22}\right] C_2^+ + \left[\frac{\alpha W}{\sqrt{6}}\mathrm{K}_{22}\right] C_2^- = 0 \tag{51}$$

and

$$-\left[\frac{\alpha W}{2}\mathrm{K}_{21}\right] C_1^+ - \left[\frac{\alpha eBa}{\sqrt{2}\hbar} I_{21}\right] C_1^- - \left[\frac{\alpha W}{\sqrt{6}}\mathrm{K}_{22}\right] C_2^+ + \left[E_{o2} - E - \frac{\alpha eBa}{\sqrt{2}\hbar} I_{22}\right] C_2^- = 0. \tag{52}$$

It also follows from Eq. (45) that $I_{12} = I_{21}$. For a nontrivial solution, the determinant of the coefficients of $C_1^+, C_1^-, C_2^+, C_2^-$ in Eqs. (49) to (52) must vanish. It can then be shown after some manipulations that

$$\begin{aligned} &X_1 X_2 - (E_{o1} - E)(E_{o2} - E)\left(S_2^- Q_1^+ + Q_1^- S_2^+\right) \\ &+S_2^+ Q_1^+\left(Q_1^- S_2^- - S_1^- Q_2^-\right) - Q_1^- S_2^- S_1^+ Q_2^+ = 0, \end{aligned} \tag{53}$$

where

$$X_1 = (E_{o1} - E)^2 - S_1^+ S_1^- \tag{54a}$$

and

$$X_2 = (E_{o2} - E)^2 - Q_2^+ Q_2^-. \tag{54b}$$

Also,

$$\begin{aligned} S_1^\pm &= \chi I_{11} \pm \frac{\alpha W}{2}\mathrm{K}_{11},\ S_2^\pm = \chi I_{12} \pm \frac{\alpha W}{\sqrt{6}}\mathrm{K}_{12}, \\ Q_1^\pm &= \chi I_{12} \pm \frac{\alpha W}{2}\mathrm{K}_{21},\ Q_2^\pm = \chi I_{22} \pm \frac{\alpha W}{\sqrt{6}}\mathrm{K}_{22} \end{aligned}$$

and

$$\chi = \frac{\alpha eBa}{\sqrt{2}\hbar}. \tag{55}$$

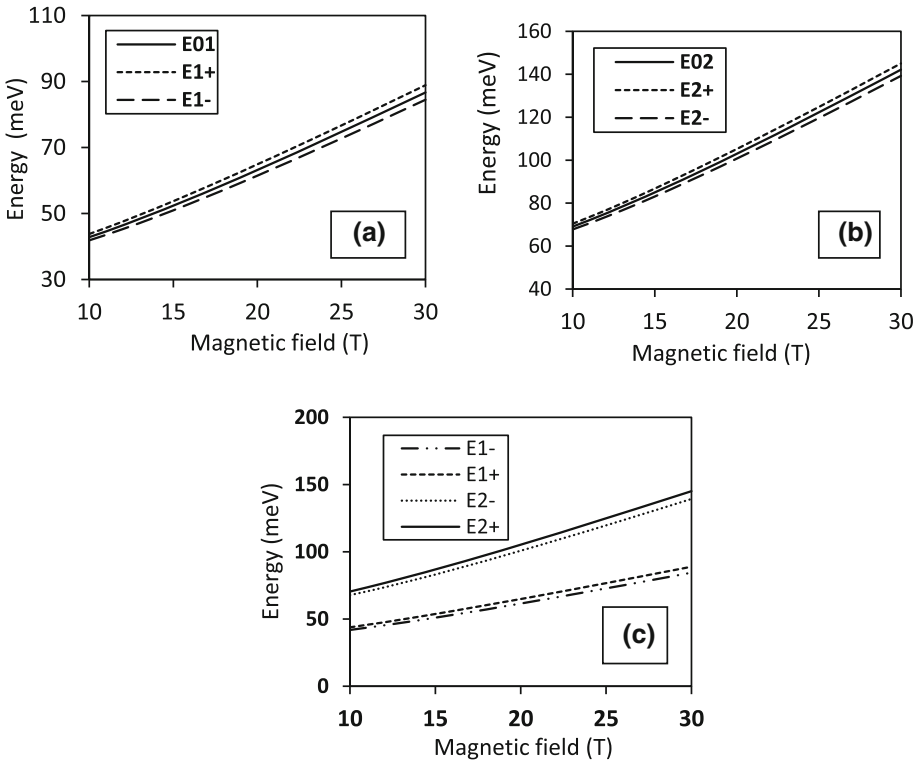

Fig. 1 Graph of the energy levels [**a** E_{o1}, $E_{1\pm})_{\text{one band}}$; **b** E_{o2}, $E_{2\pm})_{\text{one band}}$ and **c** $E_{1\pm})_{\text{two band}}$, $E_{2\pm})_{\text{two band}}$] against the magnetic field B. The values of the other parameters involved in the calculations are given by Eq. (56)

Equation (53) can be solved numerically to determine the four energy values after taking the Rashba effect into consideration. Moreover, the equation $X_1 = 0$ leads to Eq. (48) in the case of the one-band model while the equation $X_2 = 0$ leads to the analogous equation concerning E_{o2}.

6 Numerical results

The quantum dot has been taken to be a typical $GaAs$ spherical semiconductor. Accordingly

$$m^* = 0.067 m_o$$

We have investigated the variation of the Rashba effect with the applied magnetic field (B), the applied electric field (F) and the strength of the Rashba coupling coefficient (α) at a constant angular frequency (ω_o) of the parabolic confining potential.

In Fig. 1, we have started by studying the variation of the lower energy eigenvalues with the applied magnetic field in the absence and presence of the Rashba effect. We have taken

$$F = 5 \times 10^5 \text{ V/m}, \quad \omega_o = 1.5 \times 10^{13} \text{s}^{-1}, \alpha = 10^{-11} \text{eVm}. \tag{56}$$

In the absence of the Rashba effect, the two energies involved in Eq. (53) (two band model) are $E_{o1} \equiv E_{o100}$, $E_{o2} \equiv E_{o200}$. They can be determined from Eq. (16) and are displayed in Figs. 1a, b, respectively, against the applied magnetic field. Also, in Fig. 1a the two energy levels which result from the splitting of E_{o1} by taking the Rashba effect into consideration and applying the one band model ($X_1 = 0$, (Eq. 48)) have been depicted. The analogous two energy levels which result from E_{o2} are given in Fig. 1b. They are determined from the equation $X_2 = 0$. Finally, Fig. 1c is devoted to represent the four energy levels which result due to the consideration of the Rashba effect and by using the two band model (Eq. 53).

It is worthwhile pointing out that for $B \geq 6T$ the quantities $S_1^+ S_1^-$ and $Q_2^+ Q_2^-$ which appear, respectively, in the two equations $X_1 = 0$, $X_2 = 0$ are positive. Accordingly within the one band model and consequently within the two band model the energy levels which result in the range $10T \leq B \leq 30T$ considered in Figs. 1a, b, c are real.

At $B = 10T$, the two energy levels E_{o1}, E_{o2} are found from Eq. (16) to be

$$E_{o1} = 42.8369 \text{ meV}, E_{o2} = 69.0759 \text{ meV}.$$

If the Rashba effect is taken into consideration E_{o1} splits according to the one band model into the two energies

$$E_{1\pm})_{\text{one band}} = E_{o1} \pm \sqrt{S_1^+ S_1^-} \tag{57a}$$

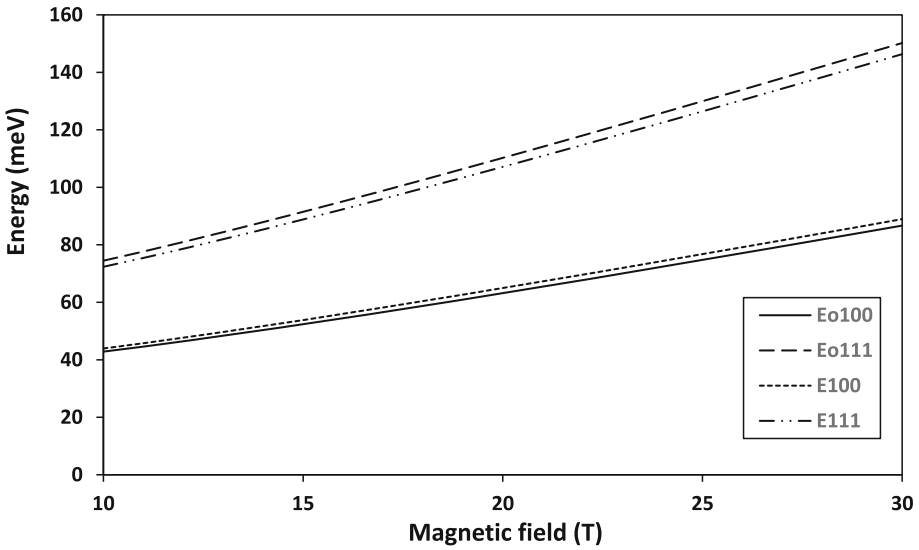

Fig. 2 Plot of the energy levels E_{o100}, E_{o111} in the absence of the Rashba effect and the energies E_{100}, E_{111} after taking the Rashba effect into account and using Eq. (40)

while E_{o2} splits into

$$E_{2\pm)\text{one band}} = E_{o2} \pm \sqrt{Q_2^+ Q_2^-} \tag{57b}$$

According to the results shown in Fig. 1a, b

$$E_{1\pm)\text{one band}} = 43.8048,\ 41.8689 \text{ meV}$$

and

$$E_{2\pm)\text{one band}} = 70.4088,\ 67.743 \text{ meV}.$$

Thus the percentage difference between $E_{1\pm)\text{one band}}$ and E_{o1} is of the order of $\pm 2.26\%$ while between $E_{2\pm)oneband}$ and E_{o2} is of the order of $\pm 1.958\%$. Also for the two band model, the first two energies $E_{1\pm)\text{two band}}$ are branched from E_{o1} while the other two energies $E_{2\pm)twoband}$ are branched from E_{o2}. The difference between the results of the two band and one band models never exceeds 1%. The results obtained over the whole range of magnetic fields considered in Fig. 1a, b, c lead to the same conclusions retrieved at $B = 10T$. It is thus clear that the consideration of models with more than two bands will not lead to any significant changes. In view of this, the other related results in the present work have been carried out by using the two-band model.

Also, the comparison with the results of Akbari et al. [37] and Shakouri et al. [38] seem to be irrelevant since in these two references the study has been performed in the presence of both Rashba and Dresselhaus interactions with fixed ratios of their coupling constants, unlike the present results which were focused on Rashba interactions. Besides, the geometry and the form of the confinement potentials differ in these references than those considered in the present work. Moreover, we preferred not to compare the results with those of Vaseghi et al. [25, 26] as the procedure they have applied seems, in our opinion, to be invalid.

In Fig. 2, we give the results obtained from Eq. (40) over the same range of magnetic field ($10T \leq B \leq 30T$). The other parameters are given in Eq. (56). In the absence of the Rashba effect, the two energies involved in Eq. (40) are $E_{o100} = E_{o1}$, E_{o111}. They have been determined from Eq. (16) and are presented in Fig. 2. The results obtained from Eq. (40) (E_{100}, E_{111}) after taking the Rashba effect into account are also given in Fig. 2. At $B = 10T$, the Rashba effect on E_{o100} and E_{o111} is of the order of 2.539% and -2.842%, respectively. The effect is of the same order over the whole range considered for B.

The variation of the lower energy levels with the strength of the Rashba coupling coefficient (α) is displayed in Figs. 3, and 4. The coefficient α varies from 0.5×10^{-11} eVm to 10^{-10} eVm. The other parameters are taken as

$$F = 5 \times 10^5 \text{ V/m}, \omega_o = 1.5 \times 10^{13} \text{ s}^{-1}, B = 10T. \tag{58}$$

In Fig. 3, the four energies $E_{1\pm)\text{two band}}$, $E_{2\pm)\text{two band}}$ which results from the two band model (Eq. 53) are depicted. We preferred here to restrict ourselves to the results of the two band model and discard those of the one band model since we are mainly interested in studying the effect of the coefficientα. Over the α range considered in Fig. 3 the energies $E_{1+)\text{two band}}$, $E_{1-)\text{two band}}$, $E_{2+)\text{two band}}$, $E_{2-)\text{two band}}$ vary by about 17.379, -23.896, 19.212, -15.798%, respectively. It is thus clear that the strength of the Rashba coupling coefficient (α) has a great effect on the energies. The increase of α by a factor of 20 has led to a change of the lower energies by about$\pm 20\%$.

In Fig. 4, the results calculated from Eq. (40) have been exhibited. The variation of α from 0.5×10^{-11} to 10^{-10} eVm has caused the solution E_{100} which has been branched from E_{o100} to increase by about 11.43%. However, the maximum value of this solution was found to be at $\alpha = 8 \times 10^{-11}$ eVm. It has been raised by about 14.05% due to the increase of α. On the other hand, the solution

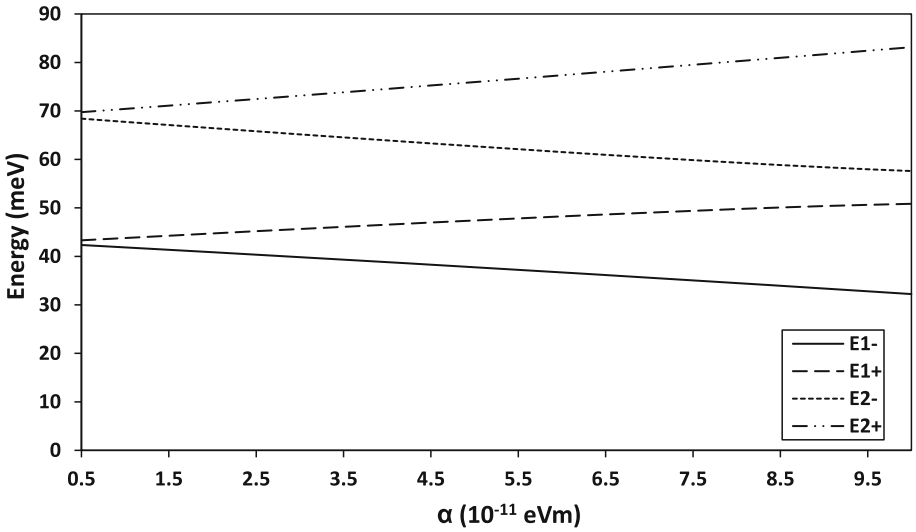

Fig. 3 Variation of the energies $E_{1\pm})_{\text{two band}}$ and $E_{2\pm})_{\text{two band}}$ with the Rashba coupling coefficient α.The energies have been calculated from Eq. (53) with the values of the other parameters given by Eq. (58)

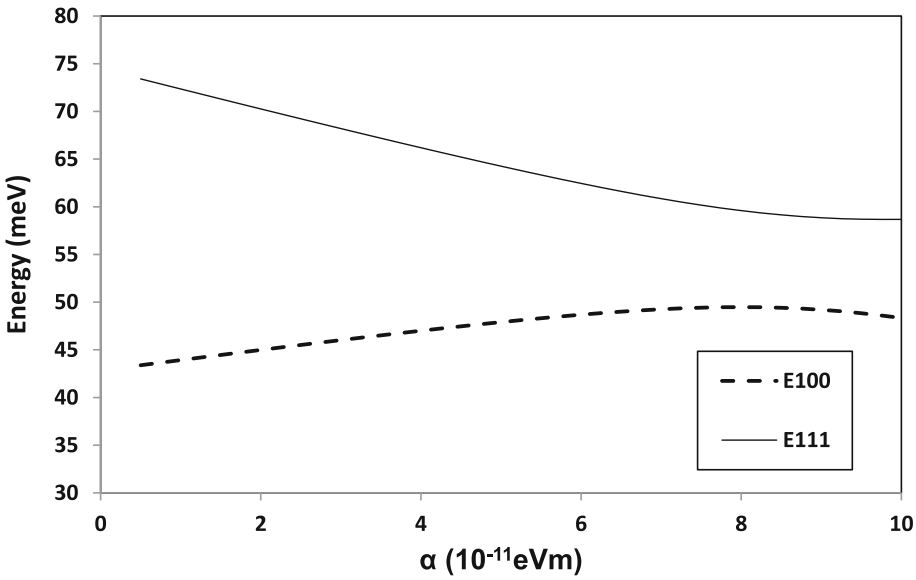

Fig. 4 Plot of the energies E_{100}, E_{111} against the Rashba coupling coefficient α. The parameters needed for the calculations are given by Eq. (58) and the energies have been calculated from Eq. (40)

E_{111} which results due to E_{o111} has continued to decrease as α increases from 0.5×10^{-11} to 10^{-10} eVm. It decreases by about 20.066%.

Finally, the variation of the lower energies due to the change of the electric field F, from 0 to 10^6V/m is displayed in Figs. 5, and 6. The other parameters have been taken as

$$\alpha = 10^{-11} \text{ eVm} \, , \omega_o = 1.5 \times 10^{13} \text{ s}^{-1}, B = 10T. \tag{59}$$

In Fig. 5, the four energies which result due to the use of the two band model (Eq. 53) have been given. Each of the energies $E_{1+})_{\text{two band}}$, $E_{1-})_{\text{two band}}$, $E_{2+})_{\text{two band}}$, $E_{2-})_{\text{two band}}$ decrease by about 5.8335 meV as F varies from 0 to 10^6 V/m. Thus the four energies vary by -12.891, -13.467, -8.116, -8.429%, respectively, over the considered range of F.

The results derived from Eq. (40) are depicted in Fig. 6. The change of F from 0 to 10^6V/m has decreased the two roots inferred from Eq. (40) by 5.8336 meV which is the same value noticed in Fig. 5. This is due to the fact that the energies calculated from Eq. (16) in the absence of the Rashba effect decrease by this value if F varies from 0 to10^6V/m. The change ofE_{o1}, E_{o2} in Eq. (53) and of E_{o100}, E_{o111} in Eq. (40) lead, in turn, to the same change in the solutions of these two equations. Thus the two roots E_{100}, E_{111} of Eq. (40) which have been branched from E_{o1}, E_{o111} vary by about -12.854%, -7.903% over the range of$F$.

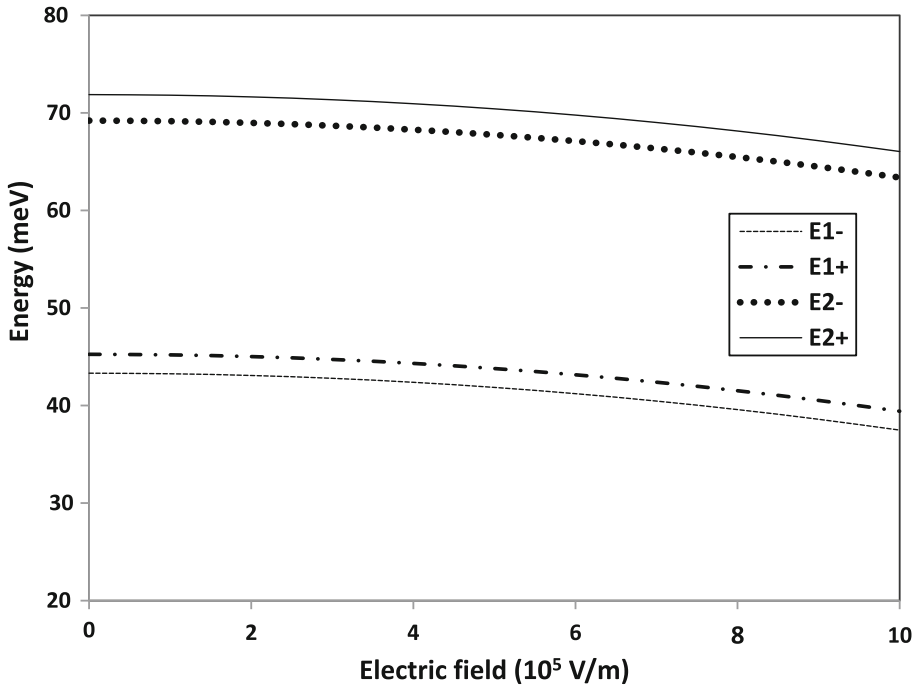

Fig. 5 Graph of the energies $E_{1\pm})_{\text{two band}}$, $E_{2\pm})_{\text{two band}}$ against the electric field F. The values of the parameters needed for the calculations are given by Eq. (59) and the energies have been calculated from Eq. (53)

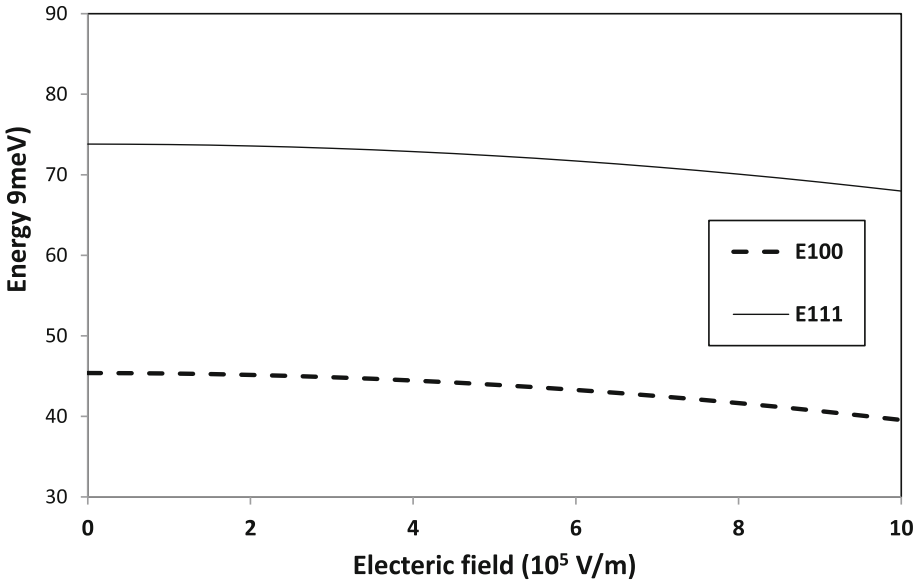

Fig. 6 Plot of the energies E_{100}, E_{111} against the electric field F. The energies have been calculated in the presence of the Rashba effect using Eq. (40). The parameters used in the calculations are given by Eq. (59)

7 Conclusions

We have dealt satisfactorily with the Rashba effect in a spherical quantum dot subject to a parabolic confining potential and external magnetic and electric fields. A new form of the wave function in the presence of the Rashba interactions has been introduced. It has been expanded in terms of all eigenfunctions of the original Hamiltonian ($\widehat{H}_o$) unlike the one used in Ref. [25] that depended only on one eigenfunction of $\widehat{H}_o$. The new form presents the exact eigenfunctions of the total Hamiltonian $\widehat{H}$ in a more accurate manner than that taken in Refs. [25, 26]. Besides, the use of an expansion gave the possibility to choose the coefficients included in alternative ways. In this connection, we have utilized two forms of these coefficients. They have been taken to depend either on the three quantum numbers involved or on the principal quantum number only. In the latter case, we have presented the one-band and the two-band models.

In all cases, the presence of the Rashba interactions has caused each energy level involved in the calculations to be splitted into two energies. The variation of the resulting energy levels has been evaluated as a function of the applied magnetic and applied electric fields and as a function of the strength of the Rashba coupling coefficient, at a fixed confining potential.

Funding Open access funding provided by The Science, Technology & Innovation Funding Authority (STDF) in cooperation with The Egyptian Knowledge Bank (EKB).

Data Availability Statement The datasets generated during and/or analysed during the current study are available from the corresponding author on reasonable request.

Declarations

Conflict of interest Here, we ensure that the authors have no competing interest to declare. Also, the manuscript does not involve any conflict statements.

References

1. D.J. Griffiths, *Introduction to Quantum Mechanics* (Pearson Prentice Hall), New Jersey, 2005)
2. R. Shankar, *Principles of Quantum Mechanics* (Plenum Press), New York, (1982)
3. I.F.I. Mikhail, I.M.M. Ismail, M.M. El Shafee, Acta Phys. Polon. A **125**, 1197 (2014)
4. I.F.I. Mikhail, I.M.M. Ismail, M.M. El Shafee, Ind. J. Phys. **90**, 1115 (2016)
5. G. Dresselhaus, Phys. Rev. **100**, 580 (1955)
6. J.D. Lu, Y.B. Li, Superlatt. Microstruct. **48**, 517 (2010)
7. B. Vaseghi, G. Rezaei, V. Azizi, F. Taghizadeh, Phys. E **43**, 1080 (2011)
8. E.I. Rashba, Sov. Phys. Solid State **2**, 1109 (1960)
9. E.I. Rashba, Phys. Rev. B **62**, R16267 (2000)
10. A. Voskoboynikov, C.P. Lee, O. Tretyak, Phys. E **10**, 107 (2001)
11. M. Florescu, S. Dickman, M. Ciorga, A. Sachrajda, P. Hawrylak, Phys. E **22**, 414 (2004)
12. Y.C. Xiao, W.J. Deng, Superlatt. Microstruct. **48**, 181 (2010)
13. P.M. Krstajic, M. Pagano, P. Vasilopoulos, Phys. E **43**, 893 (2011)
14. B. Gisi, S. Sakiroglu, K. Kasapoglu, H. Sari, I. Sokmen, Superlatt. Microstruct. **86**, 166 (2015)
15. S. Ishida, T. Manago, N. Nishizako, M. Geka, I. Shibasaki, Phys. E **42**, 984 (2010)
16. G. Gumbs, D. Huang, Phys. Lett. A **373**, 2506 (2009)
17. T.F.A. Alves, A.C.A. Ramos, G.A. Farias, R.N.C. Filha, N.S. Almeida, Eur. Phys. J. B **67**, 213 (2009)
18. W. H. Kuan, C. S. Tang, W. Xu, arXiv: cond-mat, 0403098v2 [cond–mat. mes–hall] (2004), see xxxlanl. gov
19. D.S. Kumar, S. Mukhopodhyay, A. Chatterjee, Phys. B **501**, 129 (2016)
20. S. Lahon, M. Kumar, P.K. Jha, M. Mohan, J. Lumin **144**, 149 (2013)
21. M. Kumar, S. Lahon, P.K. Jha, S. Gumber, M. Mohan, Phys. B **438**, 29 (2014)
22. M. Kumar, S. Lahon, P.K. Jha, M. Mohan, Superlatt. Microstruct. **57**, 11 (2013)
23. E. Papp, C. Micu, Superlatt. Microstruct. **48**, 9 (2010)
24. B.H. Mehdiyev, A.M. Babayev, S. Cakmak, E. Artunc, Superlatt. Microstruct. **46**, 593 (2009)
25. B. Vaseghi, G. Rezaei, M. Malian, Phys. Lett. A **375**, 2747 (2011)
26. B. Vaseghi, G. Rezaei, M. Malian, Opt. Commun. **287**, 24 (2013)
27. H. Hassanabadi, M. Solaimani, H. Rahimov, Solid State Commun. **151**, 1962 (2011)
28. M. Kumar, S. Lahon, P.K. Jha, M. Mohan, Phys. Status Solidi B **250**, 1585 (2013)
29. M. Kumar, S. Gumber, S. Lahon, P.K. Jha, M. Mohan, Eur. Phys. J. B **87**, 71 (2014)
30. P.K. Jha, M. Kumar, S. Lahon, S. Gumber, M. Mohan, Superlatt. Microstruct. **65**, 71 (2014)
31. M. Nazari, M.J. Karimi, A. Keshavarz, Phys. B **428**, 30 (2013)
32. S. Sakiroglu, B. Gisi, Y. Karaaslan, E. Kasapoglu, H. Sari, I. Sokmen, Phys. E **81**, 59 (2016)
33. A.A. Portacio, B.A. Rodriguez, P. Villamil, Phys. B **511**, 68 (2017)
34. A. Vanitha, C.W. Lee, A.J. Peter, Phys. Lett. A **375**, 208 (2010)
35. Y. Safaei, S. Davatolhagh, M.M. Golshan, Superlatt. Microstruct. **64**, 140 (2013)
36. P. Saini, A. Boda, A. Chatterjee, J. Mag. Mag. Mat. **485**, 407 (2019)
37. M. Akbari, G. Rezaei, R. Khardad, Superlatt. Microstruct. **101**, 429 (2017)
38. Kh. Shakouri, B. Szafran, M. Esmaeilzadeh, F.M. Peeters, Phys. Rev. B **85**, 165314 (2012)
39. N.N. Lebedev, *Special Functions and Their Applications* (Prentice Hall Inc., London, 1965)